Opening an Electrical Band Gap of Bilayer Graphene with Molecular Doping

Wenjing Zhang,[†,∥] Cheng-Te Lin,[†,∥] Keng-Ku Liu,[†] Teddy Tite,[†] Ching-Yuan Su,[†] Chung-Huai Chang,[‡] Yi-Hsien Lee,[†] Chih-Wei Chu,[†] Kung-Hwa Wei,[§] Jer-Lai Kuo,[‡] and Lain-Jong Li[†,⊥,*]

[†]Research Center for Applied Sciences, Academia Sinica, Taipei, 11529, Taiwan, [‡]Institute of Atomic and Molecular Sciences, Academia Sinica, Taipei, 106, Taiwan, [§]Department of Material Science and Engineering, National Chiao Tung University, Hsinchu 300, Taiwan, and [⊥]Department of Photonics, National Chiao Tung University, HsinChu 300, Taiwan. [∥] These authors contributed equally.

ABSTRACT The opening of an electrical band gap in graphene is crucial for its application for logic circuits. Recent studies have shown that an energy gap in Bernal-stacked bilayer graphene can be generated by applying an electric displacement field. Molecular doping has also been proposed to open the electrical gap of bilayer graphene by breaking either in-plane symmetry or inversion symmetry; however, no direct observation of an electrical gap has been reported. Here we discover that the organic molecule triazine is able to form a uniform thin coating on the top surface of a bilayer graphene, which efficiently blocks the accessible doping sites and prevents ambient p-doping on the top layer. The charge distribution asymmetry between the top and bottom layers can then be enhanced simply by increasing the p-doping from oxygen/moisture to the bottom layer. The on/off current ratio for a bottom-gated bilayer transistor operated in ambient condition is improved by at least 1 order of magnitude. The estimated electrical band gap is up to ∼111 meV at room temperature. The observed electrical band gap dependence on the hole-carrier density increase agrees well with the recent density-functional theory calculations. This research provides a simple method to obtain a graphene bilayer transistor with a moderate on/off current ratio, which can be stably operated in air without the need to use an additional top gate.

KEYWORDS: bilayer graphene · band gap opening · transistor · Raman spectroscopy · doping · on/off current ratio · triazine

The existence of monolayer graphene was discovered recently through mechanical exfoliation of graphite.[1] Its unique electrical, physical, and optical properties attract a variety of fundamental studies and promise many applications.[2−4] As the valence and conduction bands are degenerate at the *K* point of the Brillouin zone (named the Dirac point), graphene is known as a gapless semiconductor. The "lack of energy gap" in its electronic structure directly leads to its low on−off current ratio in transfer curves, typically <10 at room temperature.[5] Thus, *the opening of an electrical bandgap* in graphene is crucial for its application for logic circuits and photonic devices.[6,7] To break the energy degeneracy of the two electronic bands at the *K* points, various graphene superstructures with a strong quantum confinement effect, such as graphene nanoribben,[8−10] graphene quantum dots,[11,12] and graphene nanomesh[13] have been proposed. In other words, the band gap opening is expected if the graphene sheets are patterned into tens of nanometer size. It is also observed that the energy gap depends on the width and crystallographic orientation of the graphene superstructures.[14] However, reliable top-down fabrication of such small structures (<10 nm) is not possible even with state-of-the art nanolithography tools. Another possibility to induce the band gap is to break the translational symmetry of the graphene lattice.[15] Several groups have reported the presence of a band gap in monolayer graphene by using suitable underlying substrates,[16] electrical gating,[17] hydrogenation,[18−20] or putting molecules on graphene.[21−25] Optical method, angle-resolved photoemission spectroscopy (ARPES) has been used to reveal the band gap induced by molecular doping on expitaxial graphene grown on SiC substrates.[26−29] Yavari *et al.* have also indirectly observed the band gap of monolayer graphene by extracting the activation energy in temperature-variation transport for the graphene adsorbed with water molecules.[30] The band gap opening in these studies has been speculated to be a result of breaking sublattice and molecular symmetry of graphene by substrates as well as the molecular arrangement on top of graphene. Although various molecules have been used to open the band gap of monolayer graphene from 30[27] to 200 meV,[30] the on/off current ratio enhancement of the monolayer device is barely seen in the literature. It is believed that the electrical gaps obtained from the graphene layers are often smaller than their optical band gaps, suggesting that interband trapping

* Address correspondence to lanceli@gate.sinica.edu.tw.

Received for review July 4, 2011 and accepted August 6, 2011.

Published online August 08, 2011
10.1021/nn202463g

states may exist, which leads to the degradation of on/off characteristics.[31]

On the other hand, although the band structure of an ideal bilayer graphene is gapless, an energy gap can be developed in the presence of an on-site energy difference between the top and bottom layers. It has been shown that the energy gap can be generated and controlled by applying an electric displacement field using an additional gate electrode.[32−38] Similarly, an interlayer electric field can also be induced by the charge redistribution or by placing charges on the top and bottom layers, which yields the charge asymmetry between the top and bottom layers.[29] Although theoretical calculations have predicted that the band gap of a bilayer graphene can be tuned by altering the doping charge,[39] only ARPES experimental results are available.[29] Also, this doping experiment was performed in a high vacuum with an aggressive potassium dopant. In this contribution, we demonstrate that the stable organic molecule triazine can be thermally evaporated onto the top surfaces of a bilayer graphene, where the triazine molecules occupy the accessible doping on the top layer. Thus, the charge distribution asymmetry between top and bottom layers can be enhanced simply by increasing the p-doping from oxygen/moisture to the bottom layer. The on/off current ratio for a bottom-gated bilayer transistor operated in ambient conditions can be improved by at least 1 order of magnitude with triazine decoration. The estimated electrical band gap is up to ~111 meV. The observed relation between band gap and hole-carrier increase agrees with the recent density-functional theory (DFT) calculations as well as the early ARPES experiment on bilayer graphene using aggressive potassium doping.[29]

RESULTS AND DISCUSSION

Monolayer and bilayer graphenes were mechanically exfoliated from natural graphite flakes (purchased from NGS) and then transferred to 300 nm SiO_2 on highly doped Si substrates. We verified the graphene layers using Raman spectroscopy and atomic force microscopy (AFM) as previously described.[40,41] The field effect transistors were prepared by directly evaporating 1 nm of Cr and 50 nm of Au as the source and drain electrodes on top of the graphene films using hard masks. Figure 1a shows the photo of a bilayer graphene device. An organic molecule such as 1,3,5-triazine (abbreviated as triazine here) or tetracyanoquinodimethane (TCNQ) was thermally evaporated onto graphene films at 150 and 200 °C, respectively. Figure 1b schematically illustrates the setup for the evaporation process, where the molecules are placed in a vessel that is connected to another vessel for hosting graphene samples. These two vessels were initially isolated by a valve and separately pumped to vacuum for 0.5 h to remove the air in the vessels. The setup was then sealed and placed in a preheated oven. Molecules were then allowed to diffuse onto graphene surfaces after switching on the isolation valve. The evaporation period was around 8 h. Figure 1c and d show the AFM images and cross-section profiles of height for a bilayer graphene edge before and after triazine evaporation for 8 h. The increase in graphene thickness from AFM measurement demonstrates that the triazine forms a uniform thin film on graphene, and it is at least 1.25 nm thick. Note that after evaporation, some sparsely distributed triazine particles and islands are formed on the SiO_2 surfaces. To further understand the effect of molecular decoration on graphene surface, we measure the contact angle for freshly cleaved highly oriented pyrolytic graphite (HOPG) and those decorated with triazine and TCNQ, as shown in Figure 1e. The increase of hydrophobicity (increase in contact angle from 71.9° to 93.4° or 95.4°) evidences the success of molecular decoration on graphene.

Figure 2a shows the transfer characteristics (drain current I_d vs gate voltage V_g) for a bilayer graphene device before and after decorating with triazine. The on/off current ratio for the pristine bilayer is 10.8 in air, and it slightly increases to 12.4 when the measurement is performed in a vacuum of 2×10^{-5} Torr. It is noted that the on current increases but the off current decreases after decoration. This indicates that the change in graphene−electrode contact resistance, which typically results in simultaneous decrease or increase in on and off currents, is not the dominating factor. Meanwhile, the gate voltage corresponding to the charge neutrality point (V_{CNP}), the valley point in the transfer curve, is 13 V in a vacuum and it increases to 28 V in air, suggesting that the device becomes slightly more p-doped in air.[42−45] It is noted that hole (p) doping in ambient has been well explained by intrinsic graphene screening of charge at the graphene/SiO_2 substrate interface.[46,47] Moreover, Ryu *et al*. have done careful experiments and suggested that oxygen moieties withdraw electrons from graphene. Water vapor does not dope graphene noticeably, but it greatly promotes the hole doping caused by oxygen.[42] After decoration with triazine, the on/off current ratio increases to 55 measured in air, suggesting that the electrical gap is opened. Interestingly, the on/off current ratio is maximum in air (~55), and it decreases with the decreasing pressure of electrical measurement, *i.e.*, on/off ~30 at 2×10^{-5} Torr and ~20 at 3.4×10^{-6} Torr. It seems that a higher on/off current ratio is associated with a more positive V_{CNP}. Also, we observe that the increasing exposure time in pure oxygen and ambient air results in the right shifts of V_{CNP} and the enhancements of on/off current ratio (supporting Figure S2 and S3), indicating that the ambient doping from oxygen or water plays a key role in enhancing the on/off current ratio of bilayer graphene. Another

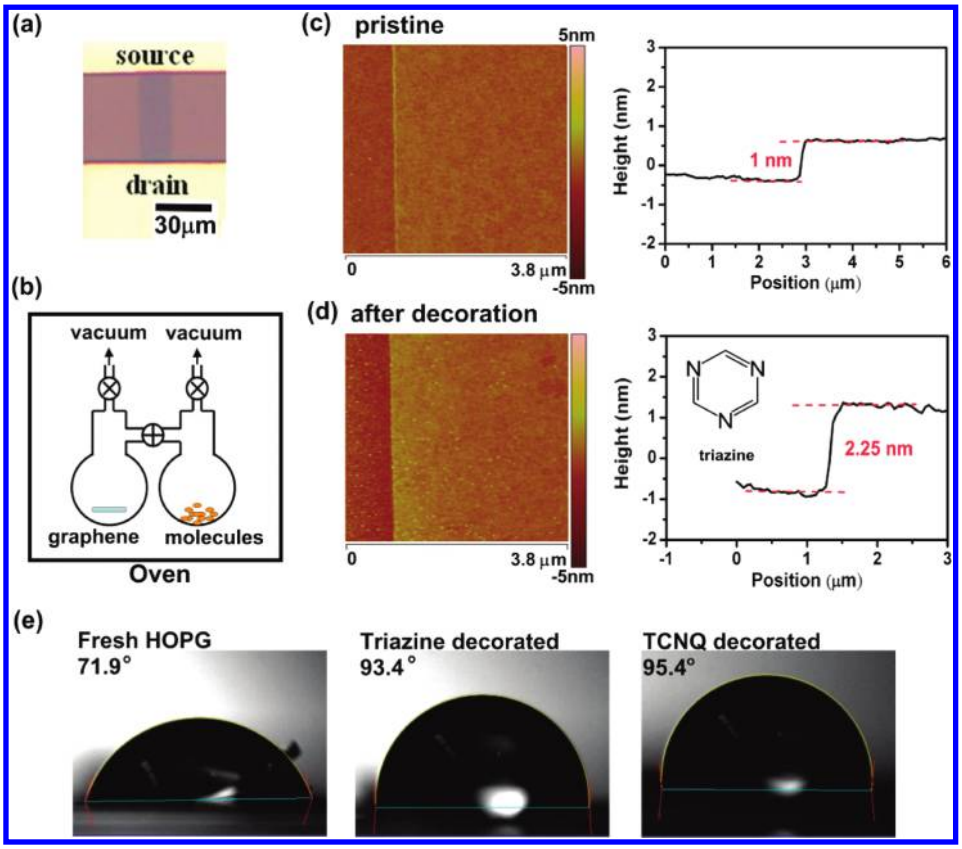

Figure 1. (a) Photo of a bilayer graphene device. (b) Schematic illustration of the setup for the evaporation process, where the molecules and graphene are placed in separate vessels connected by a valve. These vessels are placed in a preheated oven (c, d) AFM images and cross-section profiles of height for a bilayer graphene device edge (c) before and (d) after triazine evaporation at 150 °C for 8 h. (e) Contact angle results for freshly cleaved highly oriented pyrolytic graphite (HOPG) and those decorated with triazine and TCNQ.

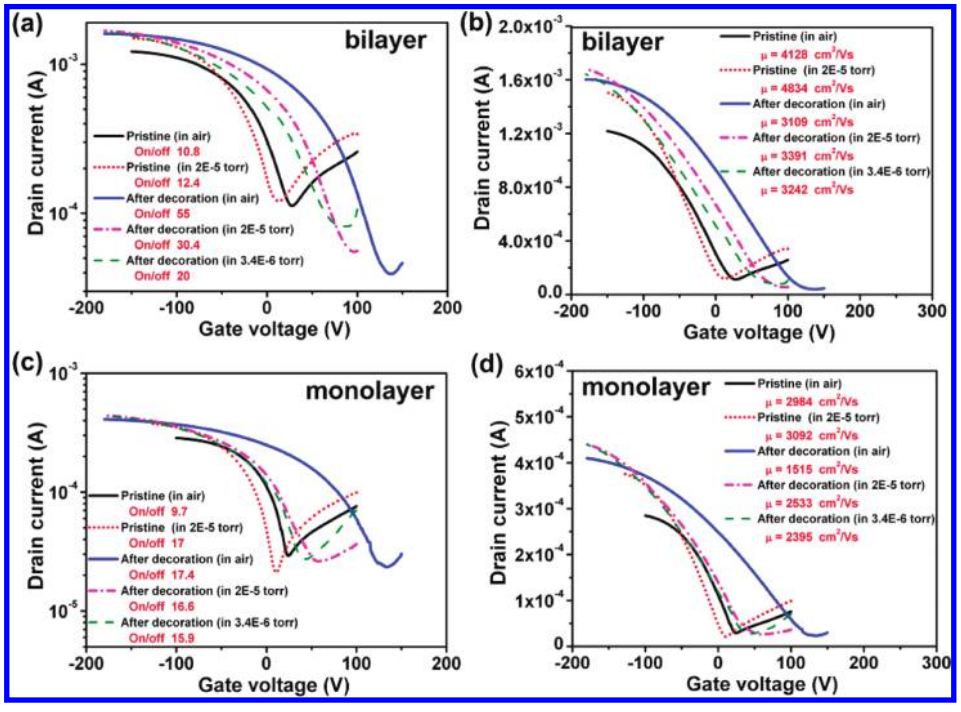

Figure 2. (a, b) Transfer characteristics (drain current I_d vs gate voltage V_g) for a bilayer graphene device before and after decorating with triazine (measured at different conditions). (c, d) Transfer characteristics for a monolayer graphene device before and after decorating with triazine.

noticeable change in transfer characteristics after triazine decoration is the decrease of field-effect hole mobility. Figure 2b replots the curves of Figure 2a to a linear scale. The field-effect mobility of holes was extracted on the basis of the slope $\Delta I_d/\Delta V_g$ fitted to the linear regime of the transfer curves using the equation $\mu = (L/WC_{ox}V_d)(\Delta I_d/\Delta V_g)$, where L and W are the channel length and width and C_{ox} the gate capacitance.[48] As expected by the impurity scattering model,[48,49] the hole mobility in air was decreased from 4128 to 3109 $cm^2/(V\ s)$ after decoration, which is likely due to charge scattering effects from the organic molecules, oxygen/moisture, and the enhanced interaction between graphene and the SiO_2 substrate caused by the thermal heating[42] in the evaporation process. Note that the values of field-effect mobility could be higher than those obtained by Hall effect measurements. Due to that, the fabrication of a Hall bar on exfoliated bilayer graphene requires the use of lithographic processes, which unavoidably introduces photoresist residues on graphene, disrupting the molecular decoration. Hence, Hall mobility measurements for the devices were not performed.

In addition, we address the fact that moisture should be present at the graphene/SiO_2 interface. Supporting Table S1 shows that the hysteresis in the transfer curves, where we define it as the gate voltage difference between the forward and reverse scans when the drain current equals (on current + off current)/2, as shown in supporting Figure S4., increases with the pressure of the electrical measurement. Shi *et al*. have reported that the oxygen adsorption does not result in hysteresis change but moisture does.[43] Thus, the hysteresis increase with doping shown in supporting Table S1 agrees well with moisture being present in the interface between bottom layer graphene and the SiO_2 substrate, as suggested by Ryu *et al*.[42]

Before we discuss the origin of the on/off current ratio increase for bilayer graphene, it is informative to see how triazine molecules affect the monolayer graphene device. For comparison, Figure 2c and d, respectively, show the logarithmic and linear scale transfer curves for a monolayer graphene device before and after triazine decoration. The on/off current ratio for the pristine monolayer device is ~10 in air, and it is ~17.4 in a vacuum of 2×10^{-5} Torr. Similar to bilayer graphene devices, the V_{CNP} for the monolayer device after triazine decoration positively shifts with the exposure to air. However, its on/off current ratio is still at around 15.9−17.4, not showing a significant enhancement. Meanwhile, the carrier mobility decreases with the triazine decoration, similar to the bilayer graphene. Note that we have performed triazine decoration on four separate monolayer graphene devices, and it is concluded that triazine decoration shows unpronounced on/off current ratio enhancement for monolayer graphene devices. Although

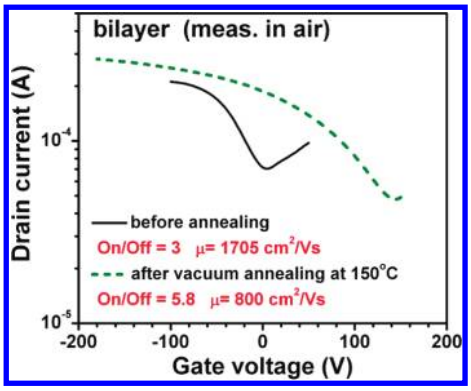

Figure 3. Ambient transfer characteristics of a bilayer graphene device before and after 150 °C thermal annealing in a vacuum of 2×10^{-5} Torr.

various molecules have been used to open the band gap of monolayer graphene,[27,30] the significant on/off current ratio enhancement of the monolayer device is barely seen in the literature. DFT calculations are used to evaluate the effect of triazine decoration on in-plane symmetry breaking of graphene. Our DFT calculations show that the band gap for the triazine-decorated monolayer graphene varies from 0.4 to 63 meV, meaning that the gap may or may not open, depending on the triazine/graphene stacking configuration (supporting Figure S5 for details). The very limited on/off current ratio increase in Figure 2c indicates that the triazine arrangement on graphene is perhaps not in a preferred stacking configuration for gap opening. Our results also suggest that the gap opening in bilayer graphene may not be from the direct in-plane symmetry breaking caused by molecular adsorption. An alternative cause is therefore taken into consideration; that is, the interlayer electric field, built up by the charge asymmetry on the top and bottom layers, can also generate an energy gap.[39] Tian *et al*. have performed detailed calculations for F4-TCNQ decoration on bilayer graphene, and they conclude that the doping effect from F4-TCNQ molecules produces a built-in electric field between the two graphene layers.[50] This interfacial electric field yields the asymmetry between the two graphene layers and results in a significant band gap opening. Hence, molecular doping effects are considered in the following paragraphs.

To further verify the role of triazine molecules on the observed electrical gap opening for bilayer graphene shown in Figure 2a, it is necessary to discuss the pure thermal heating effect because in our process the bilayer samples were heated to 150 °C during the triazine evaporation. The effect of thermal annealing on graphene has been reported.[42,51] Ryu *et al*. suggest that the effect of annealing is to clean the SiO_2 surface and to allow close coupling of graphene to the SiO_2 surface, which promotes the adsorption of oxygen and moisture to the SiO_2 surface during the subsequent exposure to air,[42] resulting in p-doping of graphene.

Figure 3 shows the ambient transfer characteristics of the bilayer graphene device before and after 150 °C thermal annealing in a vacuum of 2×10^{-5} Torr (without triazine decoration). The V_{CNP} significantly shifts to a more positive value, suggesting that the oxygen/moisture species are adsorbed at the bottom layer graphene/SiO_2 interface. The on/off current ratio of the device is also slightly increased with thermal heating, but it is not as significant as the case with triazine decoration. Figure 4a compiles the on/off current ratios for the bilayer devices before and after various treatments including triazine decoration, TCNQ decoration, and 150 °C thermal annealing in a vacuum. Supporting Figure S6 provides the typical transfer characteristics for a bilayer graphene before and after TCNQ decoration. It is clearly observed that the triazine decoration is the most promising approach for preparing higher on/off current ratio devices. By contrast, we have tested more than eight bilayer devices for TCNQ decoration. However, due to its strong p-doping nature the V_{CNP} for most of the devices is higher than 210 V, the highest gate voltage we can apply in our electrical measurement system. By considering the heavy p-doping nature of TCNQ as well as the two available TCNQ data points in Figure 4, showing a lower on/off current ratio compared with triazine, we believe that triazine is a better choice than TCNQ for enhancing on/off current ratio. Figure 4b schematically illustrates the charge distribution differences after triazine and after TCNQ decoration on the top surface of a bilayer graphene. Triazine is an electron-rich aromatic molecule due to the incorporation of N atoms in the aromatic ring, and some negative charges are expected to transfer onto the top layer graphene, while the adsorption of oxygen/moisture at the bottom layer graphene/SiO_2 interface imposes p-doping to the bottom layer graphene. Although the right shifts of V_{CNP} after triazine decoration (Figure 2) may signify p-doping, we believe the electronic doping of triazine to graphene has been overcome by the strong p-doping from oxygen/moisture caused by thermal heating in our process. To further verify the n-doping nature of triazine, we show in supporting Table S2 the Hall effect measurement results for a large monolayer graphene (size 1 cm × 1 cm; prepared by chemical vapor deposition) before and after triazine decoration, where the p-carrier concentration is decreased immediately after triazine decoration. The oxygen/moisture adsorption at the graphene/SiO_2 interface of large area graphene is slower than small exfoliated graphene; therefore, the n-doping nature of triazine is easy to observe and verify. A recent report by Wang *et al*. has used Kelvin probe force microscopy and theoretical calculations to verify that the electrical field built between top and bottom layer graphene is determined by the charge redistribution in top and bottom layer graphene.[52] In our case, the bottom layer graphene remains p-doped

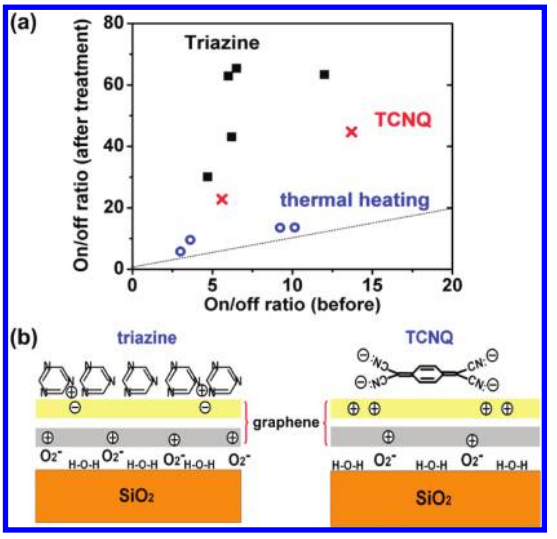

Figure 4. (a) On/off current ratios for bilayer graphene devices before and after various treatments including triazine decoration, TCNQ decoration, and 150 °C thermal annealing in a vacuum. (b) Schematic illustration for the charge distribution differences after triazine and after TCNQ decoration on the top surface of a bilayer graphene.

due to the effect of oxygen/moisture and SiO_2 substrates. Triazine and TCNQ decoration respectively imposes n- and p-doping on top layer graphene. Hence, the net electric field built after triazine decoration is large due to the doping polarity being opposite in the top and bottom layer. However, the p-doping caused by TCNQ on top layer graphene makes the bilayer device more p-doped, but the net interlayer electric field produced is smaller.

Figure 5a and b respectively show the typical Raman spectra for monolayer and bilayer graphene devices before and after triazine decoration. The position of G and 2D bands for both monolayer and bilayer graphene shifts to a higher wavenumber after decoration. Also, the intensity ratio between 2D and G bands decreases after decoration. These observations corroborate the p-doping[51] concluded from transfer curve measurements (Figure 2a and b). Figure 5c and d show the magnified G band profiles for a bilayer graphene device before and after triazine decoration, where the G band before decoration can be fitted with one Lorenzian peak, but it has to be fitted with at least two Lorenzian peaks after decoration. The observation of two G band frequencies likely suggests that the top layer and bottom graphene layers are different after decoration, *i.e*., inversion symmetry breaking.[53] For reference, the typical Raman spectra for monlayer and bilayer graphene devices before and after TCNQ decoration are shown in supporting Figure S7.

Finally, we estimate the band gap of the decorated bilayer graphene based on the on/off characteristics using Xia's method.[54] In brief, if an appreciable band gap exists, the off current of graphene transistors would be dominated by the thermionic emission.

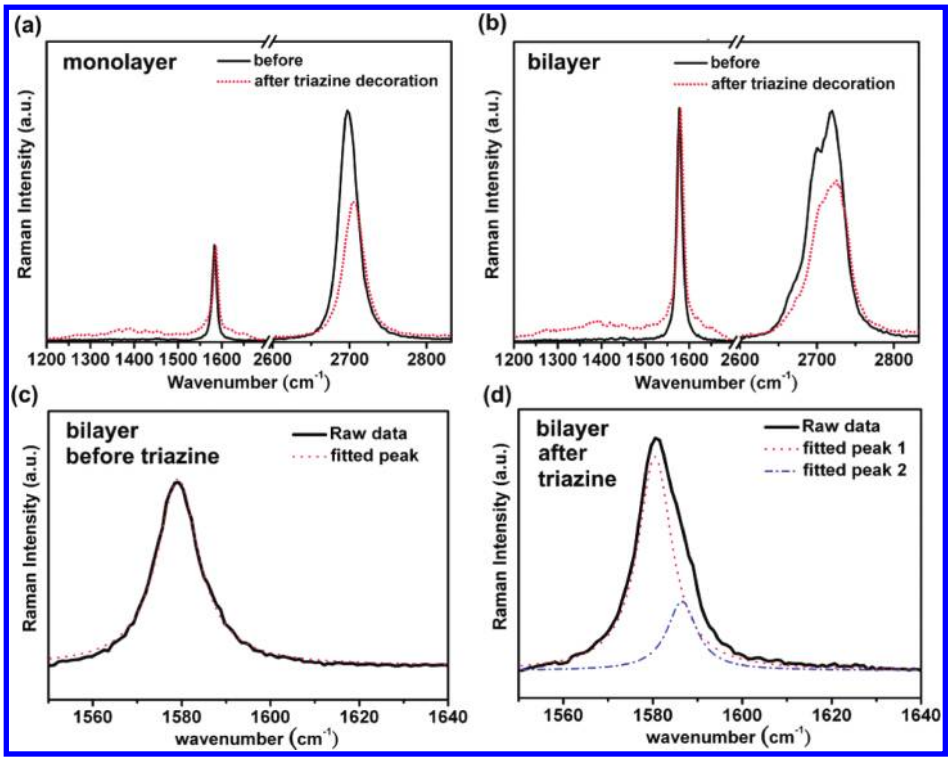

Figure 5. Typical Raman spectra for (a) monolayer and (b) bilayer graphene devices before and after triazine decoration. Magnified Raman G band profiles and corresponding Lorenzian fitting for a bilayer graphene (c) before and (d) after triazine decoration.

Therefore, the off current, I_{off}, would be proportional to $\exp(-q\ \Phi_{barrier}/k_BT)$, where q is the electron charge, $\Phi_{barrier}$ is the Schottky barrier height at the interface between the bilayer graphene and metallic electrodes, k is the Boltzmann constant, and T is the temperature. Assuming that the band gap is $E^0{}_g$ as the sample is prepared, at the charge neutral point, the Fermi level is in the middle of the energy band gap, and the increased band gap is described by

$$\Delta E_g = E_g - E^0{}_g = 2(\Phi_{barrier} - \Phi^0{}_{barrier})$$

where $\Phi^0{}_{barrier}$ is the Schottky barrier height as the sample is prepared, and E_g is the band gap after molecular decoration. So $\Delta E_g = 2(\Phi_{barrier} - \Phi^0{}_{barrier}) = (2k_BT/q)\ln(I^0{}_{off}/I_{off})$, where $I^0{}_{off}$ is the off current as the sample is prepared. The on/off current ratio for the bilayer graphene devices after triazine decoration ranges from 30 to 65, depending on the oxygen/moisture doping condition after exposure to the ambient air. The estimated band gap ranges from 36 to 111 meV based on Xia's method. As shown in Figure 2a, the on/off current ratio of the transfer curves increases with the increasing V_{CNP}. For each triazine-decorated device with a transfer curve measured under a certain doping condition, we can obtain an electrical band gap. Meanwhile, the corresponding charge impurity concentration is also obtained as $n_{imp} = (c_g/e)(V_{CNP})$,[48] where e is the electron charge and $c_g = 1.15 \times 10^{-8}$ F cm^{-2} is the gate capacitance per unit area for

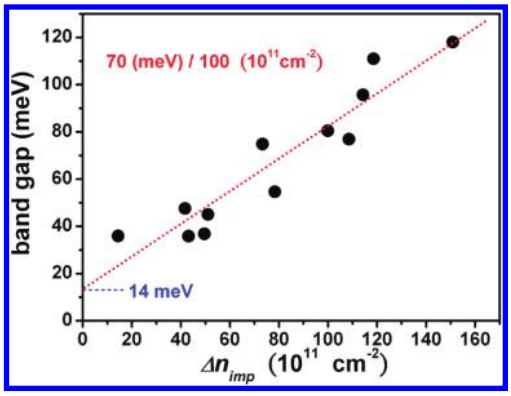

Figure 6. Estimated electrical band gap for triazine-decorated bilayer devices as a function of Δn_{imp}, where the Δn_{imp} is the charge impurity concentration difference between the triazine-decorated and its pristine form.

300 nm thick SiO_2. Figure 6 plots the relation between the electrical band gap and Δn_{imp} for each triazine-decorated bilayer device, where $\Delta n_{imp} = (c_g/e)(V_{CNP} - V_{CNP(pristine)})$ is the charge impurity concentration difference between the triazine-decorated and its pristine form. Note that the Δn_{imp} calculated here is mainly caused by the oxygen/moisture doping to the bottom layer graphene. The data points in Figure 6 demonstrate that the band gap linearly scales with the charge impurity concentration caused by ambient doping. The slope is around 70 meV/10^{13} cm^{-2}, and this result is consistent with the value ~80 meV/10^{13} cm^{-2} from the early ARPES measurement for bilayer graphene

using K as a dopant.[29] A recent DFT calculation[39] also predicts that the band gap of bilayer graphene can be modified by the electronic doping with ~80 meV increase per 10^{13} cm^{-2} increase in doping. The sloping line in Figure 6 intercepts with the *y*-axis at around 14 meV, which value is an experimental estimation for the small energy gap for the pristine bilayer graphene.

CONCLUSIONS

We have shown that the stable organic molecule triazine can be thermally evaporated and form a very uniform layer on the surface of graphene. The on/off current ratio for the bilayer graphene increases from around 10 to 30−65, and the electrical band gap is up to ~111 meV, depending on the doping concentration. The G band splitting of a bilayer graphene after triazine decoration indicates that the inversion symmetry between the top and bottom layers could be broken by the asymmetrical doping,[53] where the top layer is dominated by the triazine and the bottom layer is p-doped by ambient air. The estimated band gap linearly scales with increased charge impurity concentration. The addition of concentration $\Delta n_{imp} \approx 10^{13}$ cm^{-2} can yield a band gap of ~70 meV, which is consistent with the value ~80 meV of the potassium doping experiments[29] and theoretical calculation.[39] Comparing with the molecular decoration method, the band gap opening using an additional gate electrode may result in a larger electrical gap due to the ease of applying gate voltage. However, the fabrication of dual gate devices is not as easy as conventional single gate devices. Our proposed doping method with molecular decoration is using the same idea of breaking inversion symmetry between the top and bottom layers of bilayer graphene. The doping method is simple and the gap linearly scales with doping charge concentration. However, the gap opening is limited by the doping concentration. Thus, the selection of dopants is crucial for achieving a band gap opening.

METHODS

Device Fabrication and Transistor Measurement. The field-effect transistor device was fabricated by evaporating 1 nm of Cr and 50 nm of Au directly on top of the selected, regularly shaped graphene sheets using a copper grid (200 mesh, 20 μm spacing) as a hard mask. The typically obtained channel length between source and drain electrodes was around 20 μm. The electrical measurements were performed in ambient conditions using a Keithley semiconductor parameter analyzer, model 4200-SCS.

Characterizations. The AFM images were performed in a Veeco Dimension-Icon system. Raman spectra were collected in a NT-MDT confocal Raman microscopic system (laser wavelength 473 nm and laser spot size ~0.5 μm). The Si peak at 520 cm^{-1} was used as reference for wavenumber calibration.

DFT Calculation. We performed structural optimizations and electronic structure calculations within the framework of the density functional theory in the local-density approximation as implemented in the VASP code.[55] The energy cutoff for a plane-wave basis set is taken as 600 eV. For geometry-optimized calculation, a 12 × 12 × 1 Γ-centered Monkhorst−Pack *k*-point grid and the conjugate gradient method have been applied. All equilibrium molecule−graphene structures are obtained when all the force acting on the atoms and the axial stress are less than 0.02 eV/Å. A finer 36 × 36 × 1 *k*-point grid is used to get accurate band structure and formation energy.

Acknowledgment. This research was supported by Research Center for Applied Sciences, Academia Sinica, and National Science Council Taiwan (NSC-99-2112-M-001-021-MY3 and 99-2738-M-001-001). We also acknowledge the support from the 5y5b project of National Tsing Hua University, Taiwan.

Supporting Information Available: Supporting transfer curves, Raman spectra, and experimental details are included. This material is available free of charge *via* the Internet at http://pubs.acs.org.

REFERENCES AND NOTES

1. Novoselov, K. S.; Geim, A. K.; Morozov, S. V.; Jiang, D.; Zhang, Y.; Dubonos, S. V.; Grigorieva, I. V.; Firsov, A. A. Electric Field Effect in Atomically Thin Carbon Films. *Science* **2004**, *306*, 666–669.
2. Lin, Y.-M.; Valdes-Garcia, A.; Han, S.-J.; Farmer, D. B.; Meric, I.; Sun, Y.; Wu, Y.; Dimitrakopoulos, C.; Grill, A.; Avouris, P. Wafter-Scale Graphene Integrated Circuit. *Science* **2011**, *332*, 1294–1297.
3. Novoselov, K. S.; Geim, A. K.; Morozov, S. V.; Jiang, D.; Katsnelson, M. I.; Grigorieva, I. V.; Dubonos, S. V. Two-Dimensional Gas of Massless Dirac Fermions in Graphene. *Nature* **2005**, *438*, 197–200.
4. Liu, M.; Yin, X.; Ulin-Avila, E.; Geng, B.; Zentgraf, T.; Ju, L.; Wang, F.; Zhang, X. A Graphene-Based Broadband Optical Modulator. *Nature* **2011**, *474*, 64–67.
5. Das, A.; Pisana, S.; Chakraborty, B.; Piscanec, S.; Saha, S. K.; Waghmare, U. V.; Novoselov, K. S.; Krishnamurthy, H. R.; Geim, A. K.; Ferrari, A. C.; *et al.* Monitoring Dopants by Raman Scattering in an Electrochemically Top-gated Graphene Transistor. *Nat. Nanotechnol.* **2008**, *3*, 210–215.
6. Novoselov, K. Graphene: Mind the Gap. *Nat. Mater.* **2007**, *6*, 720–721.
7. Zhou, S. Y.; Gweon, G.-H.; Fedorov, A. V.; First, P. N.; Heer, W. A.; Lee, D.-H.; Guinea, F.; Castro Neto, A. H.; Lanzara, A. Substrate-induced Bandgap Opening in Epitaxial Graphene. *Nat. Mater.* **2007**, *6*, 770–775.
8. Brey, L.; Fertig, H. A. Electronic States of Graphene Nanoribbons Studied with the Dirac Equation. *Phys. Rev. B* **2006**, *73*, 235411–1−5.
9. Kosynkin, D. V.; Higginbotham, A. L.; Sinitskii, A.; Lomeda, J. R.; Dimiev, A.; Price, B. K.; Tour, J. M. Longitudinal Unzipping of Carbon Nanotubes to Form Graphene Nanoribbons. *Nature* **2009**, *458*, 872–877.
10. Li, X.; Wang, X.; Zhang, Li; Lee, S.; Dai, H. Chemically Derived, Ultrasmooth Graphene Nanoribbon Semiconductors. *Science* **2008**, *319*, 1229–1232.
11. Trauzettel, B.; Bulaev, D. V.; Loss, D.; Burkard, G. Spin Qubits in Graphene Quantum Dots. *Nat. Phys.* **2007**, *3*, 192–196.
12. Ponomarenko, L. A.; Schedin, F.; Katsnelson, M. I.; Yang, R.; Hill, E. W.; Novoselov, K. S.; Geim, A. K. Chaotic Dirac Billiard in Graphene Quantum Dots. *Science* **2008**, *320*, 356–358.
13. Bai, J.; Zhong, X.; Jiang, S.; Huang, Y.; Duan, X. Graphene Nanomesh. *Nat. Nanotechnol.* **2010**, *5*, 190–194.
14. Li, X.; Wang, X.; Zhang, L.; Lee, S.; Dai, H. Chemically Derived, Ultrasmooth Graphene Nanoribbon Semiconductors. *Science* **2008**, *319*, 1229–1232.

15. Mañes, J. L.; Guinea, F.; Vozmediano, A. H. Existence and Topological Stability of Fermi Points in Multilayered Graphene. *Phys. Rev. B* **2007**, *75*, 155424−1–6.
16. Giovannetti, G.; Khomyakov, P. A.; Brocks, G.; Kelly, P. J.; Brink, J. V. D. Substrate-Induced Band Gap in Graphene on Hexagonal Boron Nitride: Ab Initio Density Functional Calculations. *Phys. Rev. B* **2007**, *76*, 073103−1–4.
17. Wang, F.; Zhang, Y.; Tian, C.; Girit, C.; Zettl, A.; Crommie, M.; Shen, Y. R. Gate-Variable Optical Transitions in Graphene. *Science* **2009**, *320*, 206–209.
18. Elias, D. C.; Nair, R. R.; Mohiuddin, T. M. G.; Morozov, S. V.; Blake, P.; Halsall, M. P.; Ferrari, A. C.; Boukhvalov, D. W.; Katsnelson, M. I.; Geim, A. K.; *et al*. Control of Graphene's Properties by Reversible Hydrogenation: Evidence for Graphane. *Science* **2009**, *323*, 610–613.
19. Balog, R.; Jørgensen, B.; Nilsson, L.; Andersen, M.; Rienks, E.; Bianchi, M.; Fanetti, M.; Lægsgaard, E.; Baraldi, A.; Lizzit, S.; *et al*. Bandgap Opening in Graphene Induced by Patterned Hydrogen Adsorption. *Nat. Mater.* **2010**, *9*, 315–319.
20. Zhou, J.; Wu, M. M.; Zhou, X.; Sun, Q. Tuning Electronic and Magnetic Properties of Graphene by Surface Modification. *Appl. Phys. Lett.* **2009**, *95*, 103108-1–3.
21. Lu, Y. H.; Chen, W.; Feng, Y. P.; He, P. M. Tuning the Electronic Structure of Graphene by an Organic Molecule. *J. Phys. Chem. B* **2009**, *113*, 2–5.
22. Berashevich, J.; Chakraborty, T. Tunable Band Gap and Magnetic Ordering by Adsorption of Molecules on Graphene. *Phys. Rev. B* **2009**, *80*, 033404-1–4.
23. Dong, X.; Shi, Y.; Zhao, Y.; Chen, D.; Ye, J.; Yao, Y.; Gao, F.; Ni, Z.; Yu, T.; Shen, Z.; *et al*. Symmetry Breaking of Graphene Monolayers by Molecular Decoration. *Phys. Rev. Lett.* **2009**, *102*, 135501-1–4.
24. Zhou, S. Y.; Siegel, D. A.; Fedorov, A. V.; Lanzara, A. Metal to Insulator Transition in Epitaxial Graphene Induced by Molecular Doping. *Phys. Rev. Lett.* **2008**, *101*, 086402-1–4.
25. Huang, H.; Chen, S.; Gao, X.; Chen, W.; Wee, A. T. S. Structural and Electronic Properties of PTCDA Thin Films on Epitaxial Graphene. *ACS Nano* **2009**, *3*, 3431–3436.
26. Coletti, C.; Riedl, C.; Lee, D. S.; Krauss, B.; Patthey, L.; Klitzing, K. V.; Smet, J. H.; Starke, U. Charge Neutrality and Band-Gap Tuning of Epitaxial Graphene on SiC by Molecular Doping. *Phys. Rev. B* **2010**, *81*, 235401-1–8.
27. Zhou, S. Y.; Siegel, D. A.; Fedorov, A. V.; Lanzara, A. Metal to Insulator Transition in Epitaxial Graphene Induced by Molecular Doping. *Phys. Rev. Lett.* **2008**, 086402-1–4.
28. Zhou, S. Y.; Gweon, G.-H.; Fedorov, A. V.; First, P. N.; De Heer, W. A.; Lee, D.-H.; Guinea, F.; Castro Neto, Lanzara, A. H. A. Substrate-Induced Bandgap Opening in Epitaxial Graphene. *Nat. Mater.* **2007**, *6*, 770–775.
29. Ohta, T.; Bostwick, A.; Seyller, T.; Horn, K.; Rotenberg, E. Controlling the Electronic Structure of Bilayer Graphene. *Science* **2006**, *313*, 951–954.
30. Yavari, F.; Kritzinger, C.; Gaire, C.; Song, L.; Gullapalli, H.; Borca-Tasciuc, T.; Ajayan, P. M.; Koratkar, N. Tunable Bandgap in Graphene by the Controlled Adsorption of Water Molecules. *Small* **2010**, *6*, 2535–2538.
31. Szafranek, B. N.; Schall, D.; Otto, M.; Neumaier, D.; Kurz, H. Electrical Observation of a Tunable Band Gap in Bilayer Graphene Nanoribbons at Room Temperature. *Appl. Phys. Lett.* **2010**, *96*, 112103-1–3.
32. Zhang, Y.; Tang, T.-T.; Girit, C.; Hao, Z.; Martin, M. C.; Zettl, A.; Crommie, M. F.; Shen, Y. R.; Wang, F. Direct Observation of a Widely Tunable Bandgap in Bilayer Graphene. *Nature* **2009**, *459*, 820–823.
33. Mak, K. F.; Lui, C. H.; Shan, J.; Heinz, T. F. Observation of an Electric-Field-Induced Band Gap in Bilayer Graphene by Infrared Spectroscopy. *Phys. Rev. Lett.* **2009**, *102*, 256405-1–4.
34. Taychatanapat, T.; Jarillo-Herrero, P. Electronic Transport in Dual-Gated Bilayer Graphene at Large Displacement Fields. *Phys. Rev. Lett.* **2010**, *105*, 166601-1–4.
35. Castro, E. V.; Novoselov, K. S.; Morozov, S. V.; Peres, N. M. R.; Lopes dos Santos, J. M. B.; Nilsson, J.; Guinea, F.; Geim, A. K.; Castro Neto, A. H. Biased Bilayer Graphene: Semiconductor with a Gap Tunable by the Electric Field Effect. *Phys. Rev. Lett.* **2007**, *99*, 216802-1–4.
36. Rudberg, E.; Sałek, P.; Luo, Y. Nonlocal Exchange Interaction Removes Half-Metallicity in Graphene Nanoribbons. *Nano Lett.* **2007**, *7*, 2211–2213.
37. Son, Y.-W.; Cohen, M. L.; Louie, S. G. Half-metallic Graphene Nanoribbons. *Nature* **2006**, *444*, 347–349.
38. Kuzmenko, A. B.; Heumen, E.; Marel, D.; Lerch, P.; Blake, P.; Novoselov, K. S.; Geim, A. K. Infrared Spectroscopy of Electronic Bands in Bilayer Graphene. *Phys. Rev. B* **2009**, *79*, 115441−1.
39. Gava, P.; Lazzeri, M.; Saitta, A. M.; Mauri, F. Ab Initio Study of Gap Opening and Screening Effects in Gated Bilayer Graphene. *Phys. Rev. B* **2009**, *79*, 165431-1–13.
40. Gupta, A.; Chen, G.; Joshi, P.; Tadigadapa, S.; Eklund, P. C. Raman Scattering from High-Frequency Phonons in Supported n-Graphene Layer Films. *Nano Lett.* **2006**, *6*, 2667–2673.
41. Ferrari, A. C.; Meyer, J. C.; Scardaci, V.; Casiraghi, C.; Lazzeri, M.; Mauri, F.; Piscanec, S.; Jiang, D.; Novoselov, K. S.; Roth, S.; *et al*. Raman Spectrum of Graphene and Graphene Layers. *Phys. Rev. Lett.* **2006**, *97*, 187401-1–4.
42. Ryu, S.; Liu, L.; Berciaud, S.; Yu, Y.-J.; Liu, H.; Kim, P.; Flynn, G. W.; Brus, L. E. Atmospheric Oxygen Binding and Hole Doping in Deformed Graphene on a SiO_2 Substrate. *Nano Lett.* **2010**, *10*, 4944–4951.
43. Shi, Y.; Fang, W.; Zhang, K.; Li, L.-J. Photoelectrical Response in Single-Layer Graphene Transistors. *Small* **2009**, *5*, 2005–2011.
44. Zhang, W.; Li, L.-J. The Screening of Charged Impurities in Bilayer Graphene. *New J. Phys.* **2010**, *12*, 103037-1–6.
45. Zhang, W.; Li, L.-J. Observation of Phonon Anomaly at the Armchair Edge of Single-Layer Graphene in Air. *ACS Nano* **2011**, *5*, 3347–3353.
46. Shi, Y.; Dong, X.; Chen, P.; Wang, J.; Li, L.-J. Effective Doping of Single-Layer Graphene from Underlying SiO_2 Substrates. *Phys. Rev. B* **2009**, 115402−1–4.
47. Datta, S. S.; Strachan, D. R.; Mele, E. J.; Johnson, A. T. C. Surface Potentials and Layer Charge Distributions in Few-Layer Graphene Films. *Nano Lett.* **2009**, *9*, 7–11.
48. Chen, J. -H.; Jang, C.; Adam, S.; Fuhrer, M. S.; William, E. D.; Ishigami, M. Charged-Impurity Scattering in Graphene. *Nature* **2008**, *4*, 377–381.
49. Adam, S.; Hwang, E. H.; Galitski, V. M.; Sarma, S. D. A Self-Consistent Theory for Graphene Transport. *Proc. Natl. Acad. Sci. U. S. A.* **2007**, *104*, 18392–18397.
50. Tian, X.; Xu, J.; Wang, X. Band Gap Opening of Bilayer Graphene by F4-TCNQ Molecular Doping and Externally Applied Electric Field. *J. Phys Chem. B* **2010**, *114*, 11377–11381.
51. Ni, Z. H.; Wang, H. M.; Luo, Z. Q.; Wang, Y. Y.; Yu, T.; Wu, Y. H.; Shen, Z. X. The Effect of Vacuum Annealing on Grapheme. *J. Raman Spectrosc.* **2010**, *41*, 479–483.
52. Wang, X.; Xu, J.-B.; Xie, W.; Du, J. Quantitative Analysis of Graphene Doping by Organic Molecular Charge Transfer. *J. Phys Chem. C* **2011**, *115*, 7596–7602.
53. Yan, J.; Villarson, T.; Henriksen, E. A.; Kim, P.; Pinczuk, A. Optical Phonon Mixing in Bilayer Graphene with a Broken Inversion Symmetry. *Phys. Rev. B* **2009**, *80*, 241417(R)-1–4.
54. Xia, F.; Farmer, D. B.; Lin, Y.-M.; Avouris, Ph. Graphene Field-Effect Transistors with High On/Off Current Ratio and Large Transport Band Gap at Room Temperature. *Nano Lett.* **2010**, *10*, 715–718.
55. Kresse, G.; Furthmüller, J. Efficiency of ab-initio Total Energy Calculations for Metals and Semiconductors Using a Plane-wave Basis Set. *Comput. Mater. Sci.* **1996**, *6*, 15.